

University of Massachusetts Amherst

ScholarWorks@UMass Amherst

Environmental Conservation Faculty Publication
Series

Environmental Conservation

2021

Simulation of ecohydrological processes influencing water supplies in the Tuul River watershed of Mongolia

Javzansuren Norvanchig
University of Massachusetts Amherst

Timothy O. Randhir
University of Massachusetts Amherst

Follow this and additional works at: https://scholarworks.umass.edu/nrc_faculty_pubs




Part of the [Environmental Monitoring Commons](#), and the [Natural Resources and Conservation Commons](#)

Recommended Citation

Norvanchig, Javzansuren and Randhir, Timothy O., "Simulation of ecohydrological processes influencing water supplies in the Tuul River watershed of Mongolia" (2021). *Journal Of Hydroinformatics*. 442.
<https://doi.org/10.2166/hydro.2021.056>

This Article is brought to you for free and open access by the Environmental Conservation at ScholarWorks@UMass Amherst. It has been accepted for inclusion in Environmental Conservation Faculty Publication Series by an authorized administrator of ScholarWorks@UMass Amherst. For more information, please contact scholarworks@library.umass.edu.

Simulation of ecohydrological processes influencing water supplies in the Tuul River watershed of Mongolia

Javzansuren Norvanchig and Timothy O. Randhir ^{*}

Department of Environmental Conservation, University of Massachusetts, Amherst, MA 01003, USA

^{*}Corresponding author. E-mail: randhir@umass.edu TOR, 0000-0002-1084-9716

ABSTRACT

Achieving sufficient water supplies for multiple uses in the watershed is a major public policy issue. Understanding the current ecohydrologic processes is essential to assess potential impacts on hydrologic regimes. The Tuul River (TR) watershed faces a cold, continental climate with water supply variability. This study aims to simulate watershed processes in the TR watershed and subbasins and analyze the influences of those processes on water resources. Watershed hydrologic processes and their impact on the water resources are modeled using the Soil Water Assessment Tool (SWAT). Calibration and validation were conducted using R^2 , PBIAS, RSR, and NSE to assess the effectiveness of the SWAT model to replicate annual, monthly streamflow values. The spatial and temporal variations in watershed processes are critical for water resource decisions. With increasing uncertainty and scarcity in water resources, simulation modeling is a valuable tool in watershed management in regions with water scarcity.

Key words: ecohydrology, SWAT, Tuul River, watershed modeling, water supply

HIGHLIGHTS

- Simulates a large semiarid watershed for watershed assessment.
- Demonstrates the spatial and temporal variability.
- Models the ecohydrologic process and drivers using the SWAT model.
- Calibration and validation demonstrate model performance.
- Water resource management depends on dynamic assessment of hydrologic components.

1. INTRODUCTION

Maintaining reliable water supplies is a significant policy issue facing many countries. The uncertainty in the global climate aggravates these problems. Growing populations can accelerate the water demand, while cost-effective, supply-side options remain limited (Dharmaratna & Harris 2012). It is essential to have sufficient water for multiple uses in the watershed to have sustainable water resources. Water resources are complex systems influenced by many interacting factors like terrain, precipitation, humidity, air temperature, soil and vegetation type, land use, and land cover. Understanding the current ecohydrologic processes for a watershed is essential to assess future climate and its potential impacts on hydrologic regimes (Hongfu *et al.* 2012).

Many researchers have used different methods to assess water resources, from simple water balance equations to complex hydrological models incorporating various water resource system components. The development of accurate and informative integrated watershed models that help water managers better understand the issues within their basin currently and in the future is essential. Successful watershed models can lead to the development of timely projects for securing future water resources. Watershed modeling is a standard tool to understand a catchment's behavior under dynamic processes (Fiseha *et al.* 2013; Tsvetkova & Randhir 2019). The best model fit aims to simulate reality with minimal parameters and reduced model complexity. Watershed simulation using various parameters and equations helps predict impacts of management practices, climate, and land use (Marshall & Randhir 2008; Devia *et al.* 2015; Talib & Randhir 2017). Wang *et al.* (2021a, 2021b) used an ensemble

This is an Open Access article distributed under the terms of the Creative Commons Attribution Licence (CC BY 4.0), which permits copying, adaptation and redistribution, provided the original work is properly cited (<http://creativecommons.org/licenses/by/4.0/>).

data-driven hydrologic model to study climate boundary conditions in 16 watersheds in China. Lindenschmidt & Rokaya (2019) used a stochastic modeling approach to study ice jam flooding. Wang *et al.* (2021a, 2021b) used a clustered polynomial chaos expansion model to explore uncertainty in hydrologic prediction in the Ruihe Watershed in China.

This study simulates ecohydrological processes in a watershed with an extreme continental climate. The Soil Water Assessment Tool (SWAT) model is used to simulate the hydrologic processes of the Tuul River (TR) watershed and how those hydrological processes influence the water resources. The model is widely used for the planning and management of watersheds throughout the world. The model components include hydrology, land use, weather, crop growth, erosion/sedimentation, nutrients, pesticides, and agricultural management (Arnold *et al.* 1998). The SWAT has several advantages: (i) can simulate small to large complex watersheds (Arnold *et al.* 2012); (ii) has potential for use in ungauged or watersheds with limited monitoring data (Gassman *et al.* 2007); (iii) performs well in studies worldwide; and (iv) capable of predicting changes to water quality and quantity (Douglas-Mankin *et al.* 2010). This study is unique in applying the SWAT model to assess spatial and temporal hydrologic processes under semiarid, cold conditions in mixed-use, large river basins. The TR Basin is also less studied in literature at a watershed scale.

This study aims to simulate processes in the TR watershed and subbasins and analyze the influences of those processes on the water resources. Specifically, to: (i) model ecohydrological processes in the study watershed; (ii) analyze temporal and spatial variations in hydrologic flows; and (iii) evaluate factors influencing water supply at subbasin and watershed scales.

Alternate hypotheses are: (i) hydrological models can simulate watershed processes to reasonable accuracy; (ii) temporal and spatial variations of water flows are significant in the watershed; and (iii) specific subbasin processes impact local water supplies.

2. METHODOLOGY

2.1. Study area

The TR watershed is in Mongolia's central and northern parts (Figure 1). The watershed covers 49,994 km² and 704 km long. It flows from east to west, covering central parts of Mongolia, and is the freshwater source for its capital, Ulaanbaatar. The TR watershed has 69% rainwater, 25% groundwater, and 6% snowmelt (Dolgorsuren *et al.* 2012; Dalai *et al.* 2019).

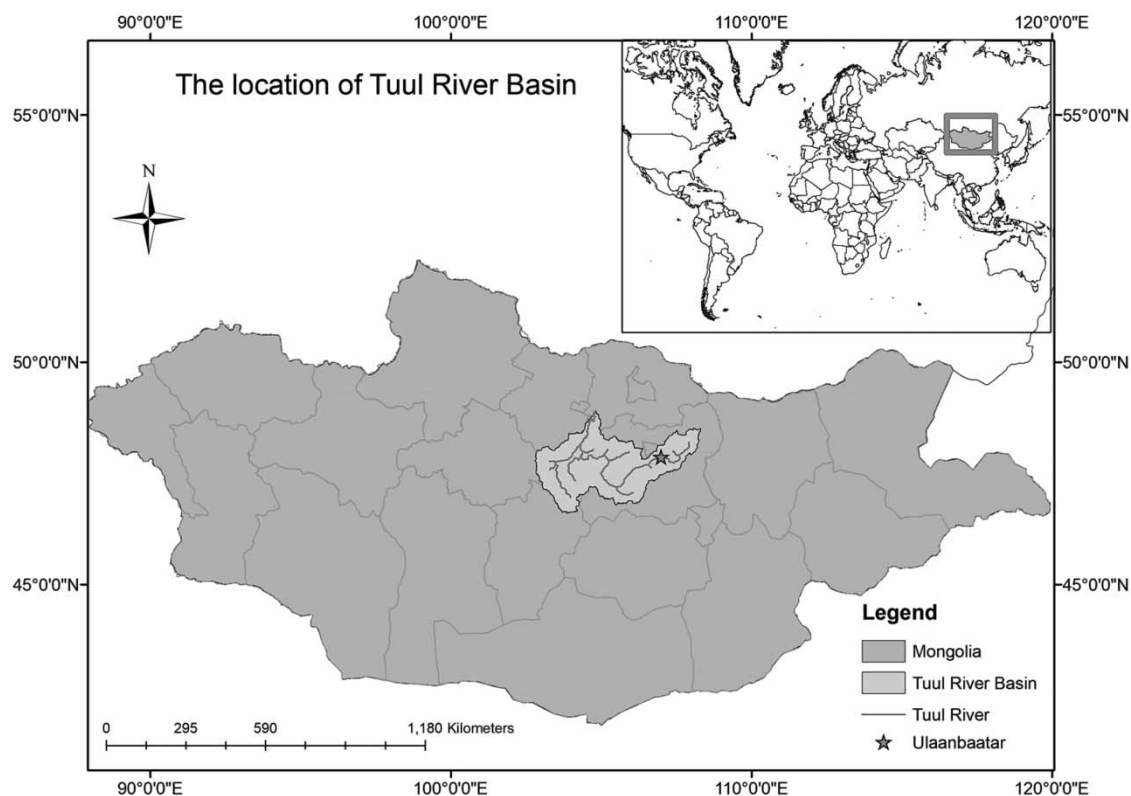


Figure 1 | Location of TR Basin in Mongolia.

The TR flows down to Ulaanbaatar from the mountain taiga and forest-steppe region. Steppes cover about 80% of the watershed. The upper river basin consists of steep rocks and forests with a valley width of approximately 1–3 km in width. Downstream of the city of Ulaanbaatar, the valley becomes broad, and the valley width expands to 8–10 km. The geographical coordinates of the point considered as the TR's origin are 108°13'20" E, 48°30'39" N, and the coordinates of the river confluence point are 104°47'52", 48°56'55" (Dolgorsuren *et al.* 2012).

The TR watershed is of high elevation surrounded by mountains with elevation ranging between 2,792 and 773 m (Figure 2). The climate is influenced by differences in day and night temperatures, long winters, and short summers. Most of the precipitation is in the summer months, dominated by warm, dry air and frequent thunderstorms. A sudden cold is observed in late August or early September, decreasing precipitation in the autumn months (Dolgorsuren *et al.* 2012).

The TR watershed has a continental climate with a wide range of temperatures, low humidity; varying precipitation; cold and long winter; and warm summer months. The rainy season (June–August) is when 90% of precipitation is received. The average annual flow in the TR at the Ulaanbaatar gaging station is 25.6 m³/s (Sukhbaatar *et al.* 2017). On the other hand, the river starts to freeze in early October until mid-April (Dolgorsuren *et al.* 2012), with a maximum ice depth of 1.16 m in mid-February (Sukhbaatar *et al.* 2017). Sukhbaatar *et al.* (2017) used the SWAT to model hydrological processes and climate change impact in the Upper TR watershed. They found that there have been cyclic variabilities such as several wet and dry periods. The latest dry period was observed during 1996–2015, where the average air temperature increased and the precipitation pattern reduced.

The average air temperature in the study area is −0.38 °C. The average temperature is from a minimum of 39.0 °C in January to a maximum of +37.20 °C in July. Warming trends are increasing by 2.0 °C from the norm in the TR watershed as observed in meteorological stations. With the increase in the number of hot days and highest temperatures since 1940 concentrating in the last decade, climate change impacts are increasing in the watershed (Sukhbaatar *et al.* 2017).

The TR watershed has an annual precipitation range from 253 to 275 mm (Sukhbaatar *et al.* 2017). Roughly 85–90% of the total precipitation is during the growing season (Dolgorsuren *et al.* 2012). In the TR watershed, the total rainfall does not change much, but rain duration is decreased during the summer. The aridity in the watershed is attributed to climate change, increasing evaporation (E), and causing aridity in the basin. With deficient water supplies to support plant cover, most areas have a low vegetative cover. The difference between evaporation and precipitation (E–P) is trending to be substantial in the last three decades.

Mountain soils evenly dominate more than 56% of the TR watershed area (Figure 3). The mountain soils include mountain dernotaiga, soddy taiga, forest dark, mountain meadow, and mountain dark chestnut soil classes. Along the river, meadow,

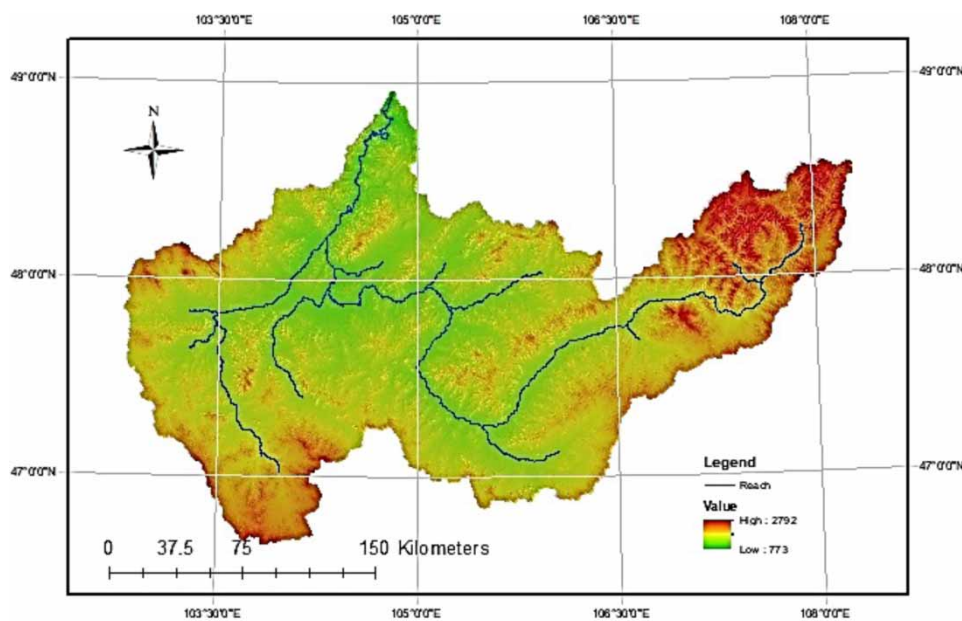


Figure 2 | Digital elevation map of the TR Basin.

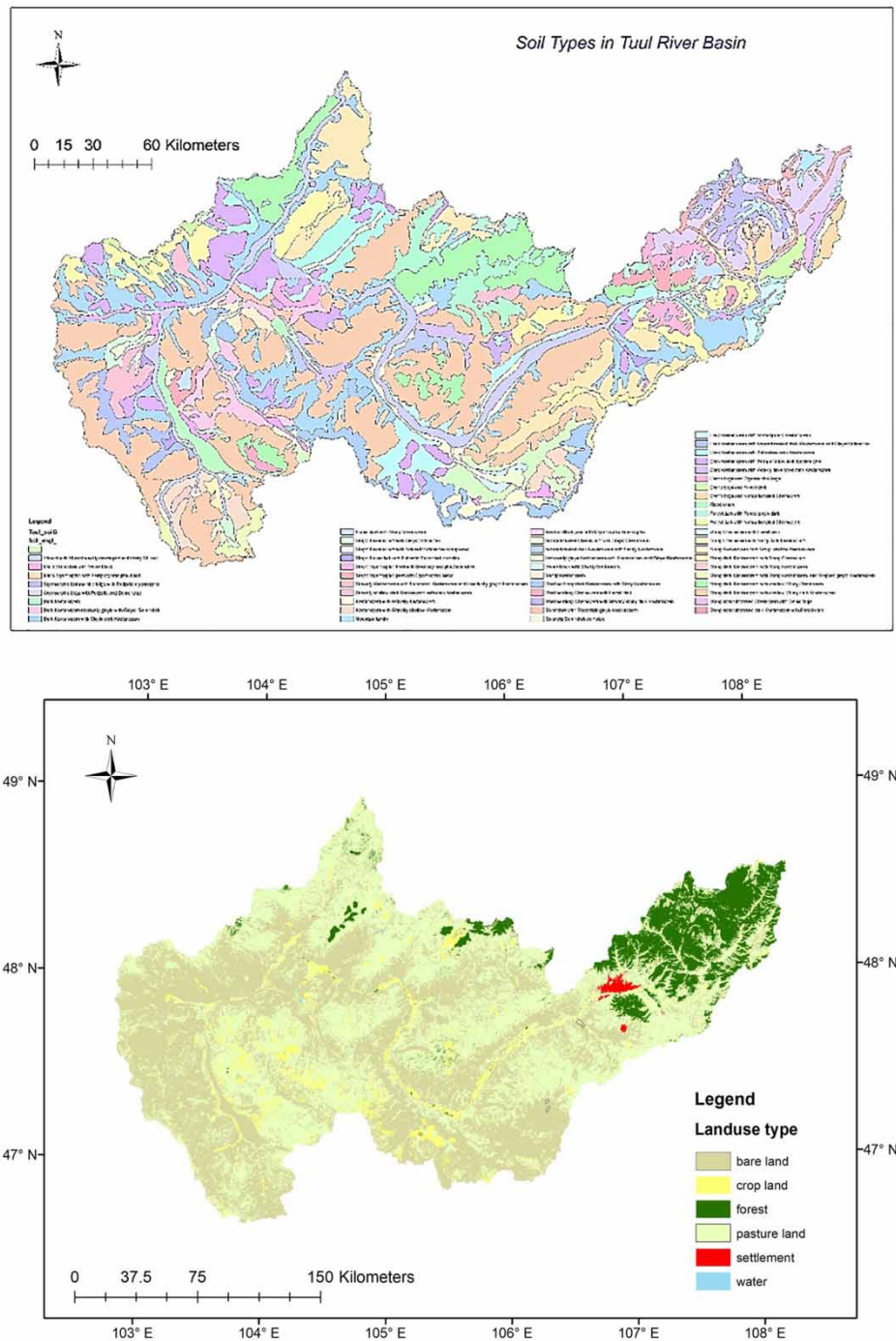


Figure 3 | Soil types and land use in the TR Basin.

swamp cryomorph, meadow cryomorph, and meadow solonchak soils are distributed. The soil types include mountain soil (56.3%), soils in steppe valley (26.2%), low hills soil (8.3%), humid region soils (6.6%), and the remaining area covered by other soils. Agriculture occupies 91.2% of the watershed, forest covers by 6.8%, and the remaining regions are settlements (Figure 3). According to the unified land classification of the Mongolian Law of Land, individual needs include agricultural land, urban and local settlement area, roads, forests, and water (Dolgorsuren *et al.* 2012).

Issues: The TR, once known for its clean and pristine water, is environmentally degraded in the last several decades. The river is the primary source (94%) of recharge to the alluvial aquifer (Tsumijima *et al.* 2013). It is the primary source of drinking

water to the city of Ulaanbaatar, the capital of Mongolia. Therefore, water sources and the river flow are the most important to the city's estimate 2021 population of 1.6 million residents (UN 2019). Over the past two decades, the river is facing low flows and declining groundwater levels. The TR watershed faces some critical issues regionally. The Upper TR watershed is forested and has issues regarding deforestation due to the expansion of tourism and camping. The Middle TR watershed downstream of the Ulaanbaatar city is highly polluted with poorly treated wastewater discharged from Waste Water Treatment Plant. In addition, there have been issues regarding the overgrazing of livestock and pollution from the Zaamar gold mine in the lower TR watershed (Dolgorsuren *et al.* 2012). Several studies have assessed the water resources in the headwaters (Sukhbaatar *et al.* 2017) and groundwater abstraction (JICA 2010; Tsujimura *et al.* 2013). However, subbasin and river basin-level analyses were not conducted for watershed management.

2.2. Conceptual model

A methodological framework (Figure 4) shows hydrological components (runoff, infiltration, subsurface, groundwater, and evapotranspiration) used in this study. The framework includes data collection, pre-processing, calibration, validation, model performance, and simulation of the hydrological components.

Hydrological models are commonly used to understand a watershed system and its hydrological processes better. The SWAT is a comprehensive model to provide a detailed analysis of water resources and easy to modify any changes to the system (Arnold *et al.* 1998). The SWAT model has been increasingly and successfully used worldwide for various purposes, e.g., assessing water resources, planning, and management, studying hydrologic impacts of climate or land-use changes (Ficklin *et al.* 2013) from global to local scales. The SWAT is an ecohydrologic model (Devia *et al.* 2015) useful in studying the effect of management and climate on water resources. The model segments the simulation area into subwatersheds and hydrological response units (HRUs) that incorporate unique land-use, soil attributes (Abouabdillah *et al.* 2014). It uses daily meteorological inputs to replicate the watershed mechanisms; the output could be summarized monthly or yearly for an extended simulation period. The SWAT model is also commonly used to simulate ungauged watersheds as there are many countries where hydrological and meteorological monitoring is limited.

The SWAT model has vast applications and is widely used worldwide for the assessment of water resources (Dessu *et al.* 2014; Jujnovsky *et al.* 2017), water quality (Abbaspour *et al.* 2015; Fan & Shibata 2015), land-use changes (Wang *et al.* 2014; Krysanova & Srinivasan 2015; Neupane & Kumar 2015; Sajikumar & Remya 2015), and climate change (Johannsen *et al.* 2016; Faramarzi *et al.* 2017).

Although the SWAT can require many inputs to simulate the hydrological process, it has been successfully applied in data-limited studies and is a feasible and valuable approach for strengthening water resources management (Niu *et al.* 2014; Fukunaga *et al.* 2015).

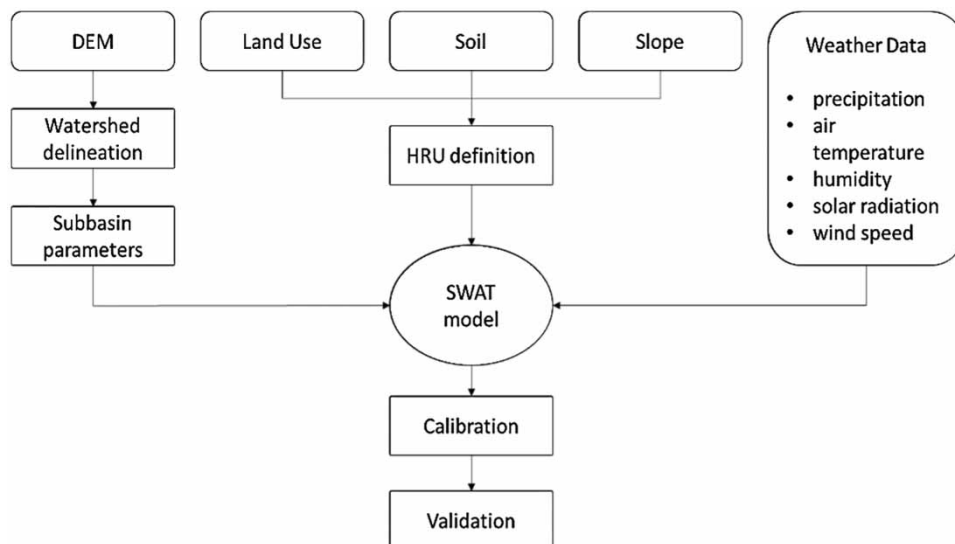


Figure 4 | Conceptual model.

The following hydrological components were used to simulate the hydrology of the study watershed. The water balance equation is represented by $SW_t = SW_0 + \sum_{i=1}^t (R_i - Q_i - ET_i - P_i - QR_i)$, in which SW_t and SW_0 are soil water at the beginning and end of the day i , t is the time interval in days, and R , Q , ET , P , and QR represent precipitation, runoff, ET, percolation, and return flow, respectively. The SCS curve number equation, $Q = (R - 0.2s)^2 / (R + 0.8s)$, is used for predicting surface runoff (USDA-SCS 1972). Where Q , R , and s are runoff (mm), rainfall (mm), and a retention parameter that varies (1) with watershed because of land use, soil, management, and slope all range and (2) over time variation of soil water content. The retention parameter is associated with the curve number (CN) in the SCS formula (Arnold *et al.* 1998). The percolation is modeled as a storage routing technique, integrated with a crack-flow model, to simulate flows through each soil layer. Percolating water enters groundwater as a return flow downstream. The storage routing is based on $SW_i = SW_{ei} \exp(-\Delta t / TT_i)$, in which SW_0 and SW are the soil water content at the beginning and end of a day, Δt is the time-step (24 h), and TT is time (h) through layer I (Arnold *et al.* 1998). The percolation rate (mm d^{-1}) is calculated as $O_i = SW_i [1 - \exp(-\Delta t / TT_i)]$. In the soil profile from 0.0 to 2 m, lateral subsurface flow is estimated along with percolation. A kinematic storage model calculates the lateral flow in each soil layer. Return flow from the shallow aquifer to the stream is calculated as $q_{\text{lat}} = 0.024(2 S \text{ SCsin}(\alpha)) / \theta_d L$ (Arnold *et al.* 2000). Where q_{lat} is the lateral flow (mm d^{-1}), S is the volume of soil water (m h^{-1}), α is the slope (mm^{-1}), θ_d is the drainage porosity (mm^{-1}), and L is the flow length (m) (Arnold *et al.* 1998).

This study uses Penman–Monteith method (Monteith 1965) for estimating potential evapotranspiration (PET). Exponential functions of soil depth and water content are used for predicting soil evaporation, and a linear function of PET and leaf area index is used for simulating plant water evaporation (Arnold *et al.* 1998). When the soil second-layer temperature is simulated more than 0.0°C , snow may be melted, which is simulated as $\text{SML} = T(1.52 + 0.54\text{SPT})$, where SML is the rate of snow-melt (mm d^{-1}), SPT is the snowpack temperature ($^\circ\text{C}$), and T is the average daily temperature ($^\circ\text{C}$). In many semiarid regions, river flow and streamflow are hydraulically linked with alluvial floodplain groundwater. Transmission is simulated using Lane's method (USDA 1983) to simulate losses as flood wave travels downstream (Arnold *et al.* 1998).

2.3. Data collection

Data used in modeling include climate (rainfall, air temperature), hydrologic processes (flow rate), and spatial (topography, land use, soil). The type and sources of the data used in this study are provided in Table 1.

2.4. Model construction

The ecohydrological model for the entire TR watershed and its subwatersheds was developed in this study based on the available data. The SWAT is used to simulate hydrological processes in the watershed.

As it has been widely used in scarce data watersheds to simulate various processes in watersheds, the SWAT model is selecting to simulate and understand the ecohydrological processes in the TR watershed. The SWAT model was previously used for two watersheds in Mongolia. The effect of subarctic conditions on the Kharaa river basin, located in the northern part of Mongolia, was simulated using the SWAT model. It was found that SWAT satisfactorily reflects streamflow for particular years but is not reliable for a more extended period (Hülsmann *et al.* 2015). Sukhbaatar *et al.* (2017) developed the SWAT model for the Upper TR watershed to analyze the impact of climate change on hydrological processes. They found

Table 1 | Data types and their sources

Data type	Source
Temperature, precipitation, humidity, wind speed, streamflow	National Agency for Meteorology, Hydrology and Environment Monitoring (NAMHEM)
Solar radiation	MWSWAT Global weather station data
DEM	Advanced Spaceborne Thermal Emission and Reflection Radiometer (NASA JPL 2009).
Soil type	Harmonized World Soil Database from FAO
Land use	The GlobCover initiative of the ESA
River basin boundary, river network	Tuul River Basin Authority

that the model sufficiently predicted the hydrological processes in the watershed and further concluded that the river flow was primarily influenced by precipitation.

The TR watershed was analyzed based on the HRU that represents homogeneity in land and soil characteristics. Water resources for the TR watershed were simulated from 1996 to 2011 using observed precipitation, temperature, wind speed,

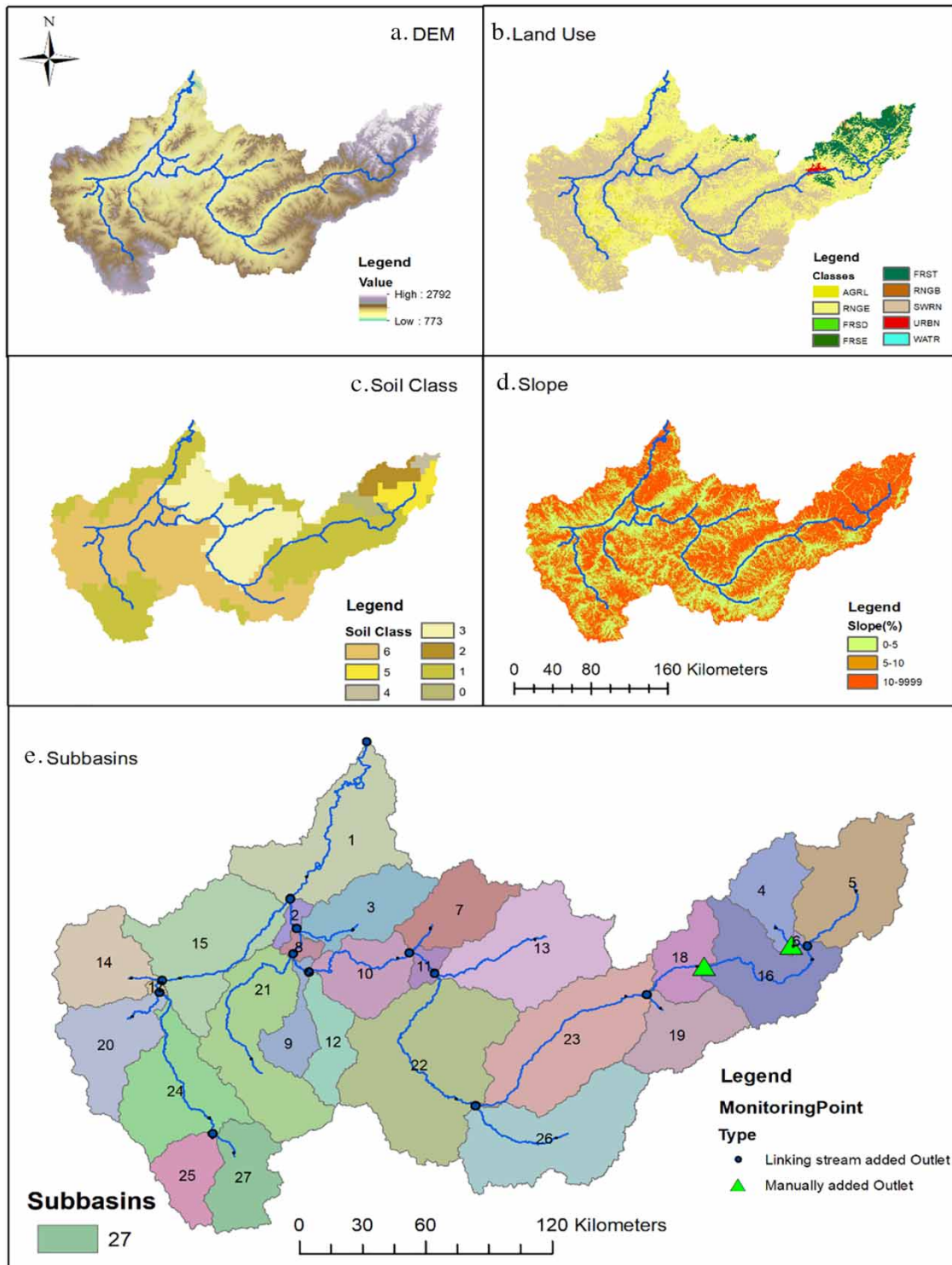


Figure 5 | SWAT model inputs. (a) DEM, (b) land use, (c) soils, (d) slope and (e) subbasins.

and air humidity inputs. The streamflow data from two stations (Ulaanbaatar and Terelj) in the watershed are used to calibrate and validate SWAT model results.

The SWAT model was developed using the topography, land use, soil, and meteorological data from the TR watershed. SWAT parameters were derived from spatial analysis of the watershed using GIS and procedures suggested in the SWAT manual. Spatial inputs to the SWAT model (Figure 5) include (a) topography, (b) land use/cover, (c) soil class, (d) surface slope, and (e) subbasins. The global digital elevation model, generated from satellite imagery using an Advanced Spaceborne Thermal Emission and Reflection Radiometer (NASA JPL 2009), was used. The topography has a resolution of 30×30 m. Land-use/cover data of the European Space Agency (ESA) was used in modeling. The GlobCover initiative of ESA uses the Envisat MERIS data of Fine Resolution (300 m) (Arino *et al.* 2012; Sukhbaatar *et al.* 2017). The soil map is from the Harmonized World Soil Database from FAO (Food and Agriculture Organization). The TR watershed is divided into 27 subwatersheds based on the unique HRUs (Figure 5).

2.5. Calibration and validation

Calibration and validation of the SWAT model performed using the coefficient of determination (R^2), RMSE of observations standard deviation ratio (RSR) (Moriassi *et al.* 2007), and Nash–Sutcliffe model efficiency (NSE) (Nash & Sutcliffe 1970). The R^2 is the degree of agreement between simulated and measured data, measured as $R^2 = \left[\sum_i (Q_{m,i} - \bar{Q}_m)(Q_{s,i} - \bar{Q}_s) \right]^2 / \sum_i (Q_{m,i} - \bar{Q}_m)^2 \sum_i (Q_{s,i} - \bar{Q}_s)^2$, where Q is the dependent variable, and m and s stand for observed and simulated for i^{th} data pair. Higher values of R^2 indicate higher explanatory power. NSE determines the relation between residual variance compared with measured variance. $NSE = 1 - \sum_i (Q_m - Q_s)_i^2 / \sum_i (Q_{m,i} - \bar{Q}_m)^2$, where the bar represents an average value. NSE ranges between $-\infty$ and 1, with an optimal value of $NSE = 1$.

The $RSR = \sqrt{\sum_{i=1}^n (Q_m - Q_s)_i^2} / \sqrt{\sum_{i=1}^n (Q_{m,i} - \bar{Q}_m)^2}$ varies from 0 to large positive values, with lower values of RSR indicating a better model fit (Moriassi *et al.* 2007).

Santhi *et al.* (2001) suggest that the SWAT calibration results are acceptable of R^2 and NSE. In addition to that, Moriassi *et al.* (2007) also summarized the overall performance rating for recommended statistics for monthly time-step (Table 2).

The SWAT model calibration was conducted using the SWAT-CUP (SWAT-Calibration Uncertainty Procedures) program. SWAT-CUP is designed for calibration and validation, sensitivity, and uncertainty analyses of SWAT results (Arnold *et al.* 2012; Abbaspour *et al.* 2015; Boithias *et al.* 2017). SWAT-CUP analysis and Sequential Uncertainty Fitting version 2 (SUFI2) algorithm (Abbaspour *et al.* 2007) were used for sensitivity analysis and calibration. The sensitive analysis was conducted to assess the influence of parameters on river flow prediction in the SUFI2 algorithm. Other methods for sensitivity analysis used in hydrologic studies include the Generalized Likelihood Uncertainty Estimation (GLUE) algorithm (Beven & Binley (1992) and statistical factorial methods (Wang *et al.* 2020). SUFI2 was found superior to GLUE in runoff simulations in forest watersheds (Nohegar *et al.* 2017). The obtained model is calibrated and validated using daily streamflow data from two hydrological gauges (Terelj and Ulaanbaatar stations) in the headwaters. The models' calibration and validation were conducted using the same period with two gauging stations available in the watershed. The model was calibrated with 1990–2011 data using the discharge data from the Ulaanbaatar station using statistical methods listed in Table 2. The model validation was conducted using the Terelj station data ranging from 1990 to 2011 as internal validation.

3. RESULTS AND DISCUSSION

The SWAT model simulated the hydrological processes in each subwatershed for 25 years (1987–2011). The results are compiled for daily, monthly, and yearly values of flows. Daily values had low validation and calibration values. This was due to

Table 2 | Performance criteria for parameters (Moriassi *et al.* 2007)

Performance	R^2	NSE	RSR
Very good	>0.6	$0.75 < NSE \leq 1$	$0.0 \leq RSR \leq 0.5$
Good		$0.65 < NSE \leq 0.75$	$0.5 \leq RSR \leq 0.6$
Satisfactory		$0.50 < NSE \leq 0.65$	$0.60 \leq RSR \leq 0.7$
Unsatisfactory	<0.6	$NSE \leq 0.50$	$RSR > 0.7$

missing and limited observed values. Therefore, the initial three years are used for the warm-up. From model results, only annual and monthly average basin values were used to study seasonality and yearly trends in water balance components for every 27 subwatersheds.

The calibration results for the monthly time-step using the simulated and observed discharge data values at Terelj and Ulaanbaatar stream (Table 3). The statistical values for calibration and validation were good (R^2 , NSE, and RSR) and satisfactory (PBIAS) (Moriassi *et al.* 2007).

The parameter global sensitivity analysis is conducted in the SUFI2 by regressing a Latin hypercube generated parameters against the objective function (Khalid *et al.* 2016). The most sensitive parameters are SOL_AWC(1).sol, GW_DELAY.gw, SOL_K(1).sol, ESCO.hru, CH_N2.rte, and CH_K2.rte. (Figure 6). The available watershed capacity (SOL_AWC) is a major factor in semiarid regions that influence the vegetative cover, water uptake, and runoff generation. The time of vadose zone flow past the lowest depth (GW_DELAY) is sensitive as this subsurface flow rate is influential in semiarid, cold climate watersheds. The saturated hydraulic conductivity (SOL_K) in layer 1 influences the rate of flow of water in the soil, which is critical in influencing runoff, subsurface flows, infiltration, and stream discharge. The soil evaporation compensation factor (ESCO) defines the soil evaporative demand and influences soil water through subsurface loss in water that influences the balance in subsurface flows. The channel parameters in the TR (CH_N2 and CH_K2) are sensitive given the variability in geomorphology and in-channel processes (Pietroń *et al.* 2015).

The observed and simulated monthly streamflow values at Terelj and Ulaanbaatar stations are shown in Figure 7. The average annual water balance components in the TR Basin are: precipitation = 277.5 mm, surface runoff $Q = 0.44$ mm, lateral soil flow = 58.14 mm, groundwater (shallow aquifer) $Q = 4.50$ mm, groundwater (deep aquifer) $Q = 0.24$ mm, revap (shallow aquifer \geq soil/plants) = 0.66 mm, deep aquifer recharge = 0.24 mm, total aquifer recharge = 4.73 mm, total water yield = 63.31 mm, percolation out of soil = 4.73 mm, ET = 214.3 mm, PET = 696.0 mm, and total sediment loading = 0.16 t/ha. The model simulated precipitation = 277.5 mm and snowfall = 46.26 mm, which fall within the range reported by Dolgorsuren *et al.* (2012) and Sukhbaatar *et al.* (2017). Moreover, the TR watershed average has 45.15 annual basin water stress days and 133.79 temperature stress days.

Table 3 | Calibration and validation results

	R^2	NSE	RSR
Ulaanbaatar (calibration)	0.66	0.66	0.58
Terelj (validation)	0.70	0.66	0.59

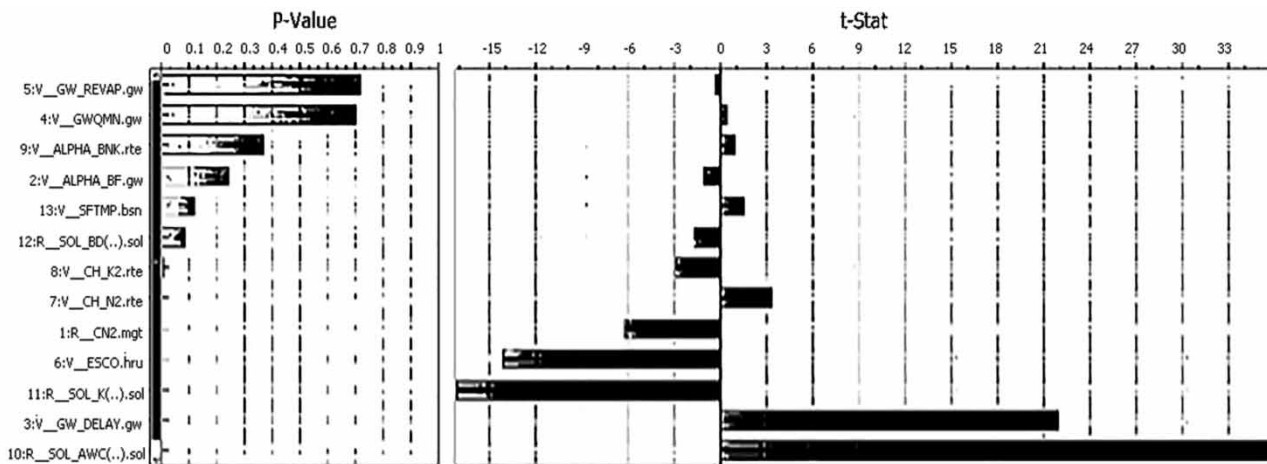


Figure 6 | Global sensitivity of calibrated parameters.

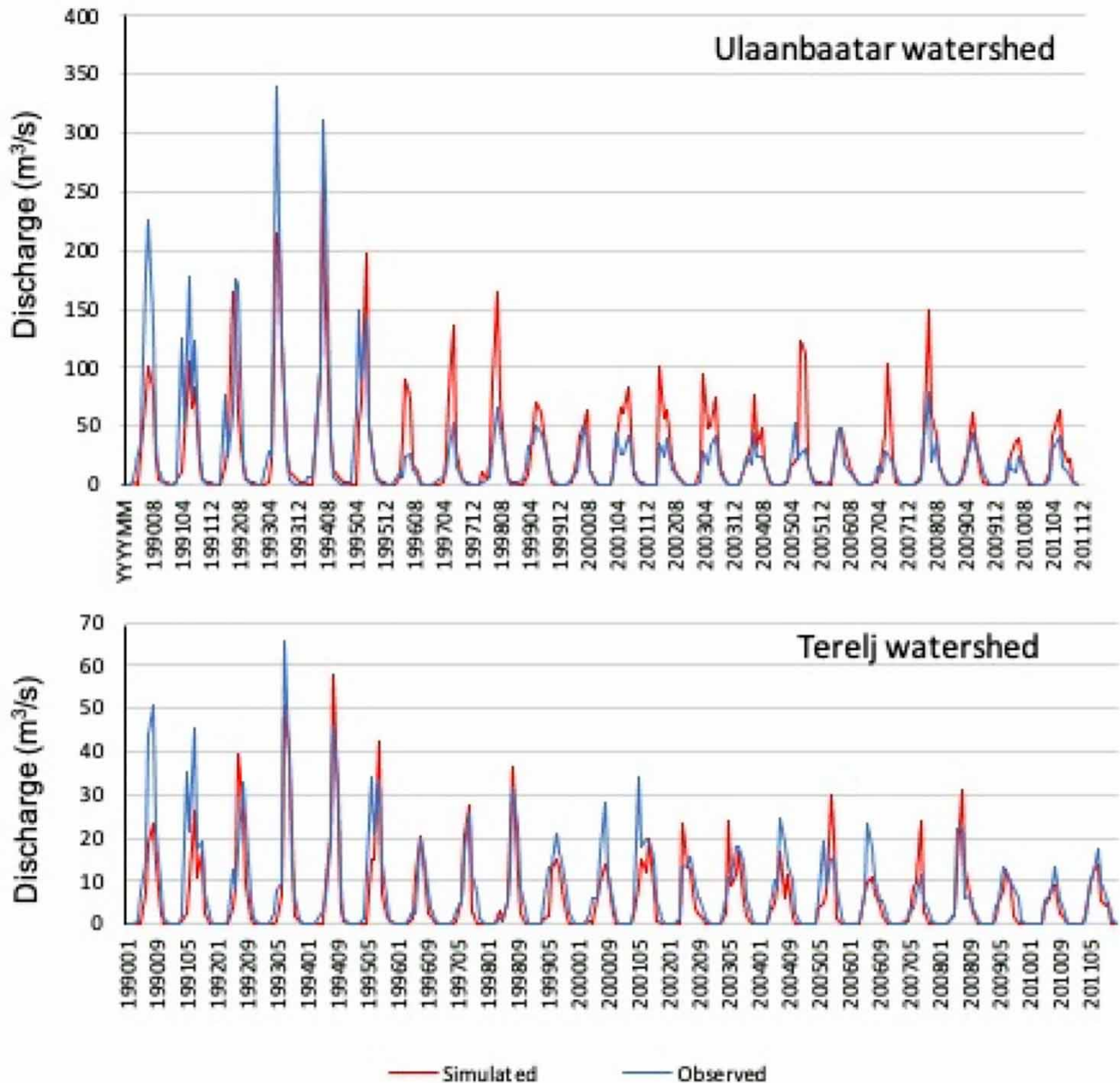


Figure 7 | Observed and simulated streamflow at Terelj and Ulaanbaatar stations.

The average monthly basin values are calculated and shown in Figure 8. The maximum amount of rain is simulated in July at 76.16 mm. The maximum amount of surface runoff was 0.12 mm in August when the lateral flow (16.43 mm) and water yield (17.74 mm) were also the highest. The lowest value of precipitation was observed in January. The average annual water yield was 63.31 mm. The seasonal flows show a typical water balance among the months.

Some variations are observed between the actual and potential ET measurements. This is due to input variables in Hamon PET that are based on day length and air temperature only. In contrast, actual ET is influenced by additional factors such as solar radiation, relative humidity, and wind speed. The changes in ET are directly correlated to the growing season and type of vegetation in the watershed. The ET gradually decreases from September to January, as deciduous trees lose their leaves, reduced demand for ET in September–October, and drop in air temperature. As the dormant season starts, the ET decreases and reaches a minimum in January. This is because of snow cover accumulating on evergreen trees and the ground. As days get warmer in spring and day length increases, ET also increases, starting in February. When the growing season begins in

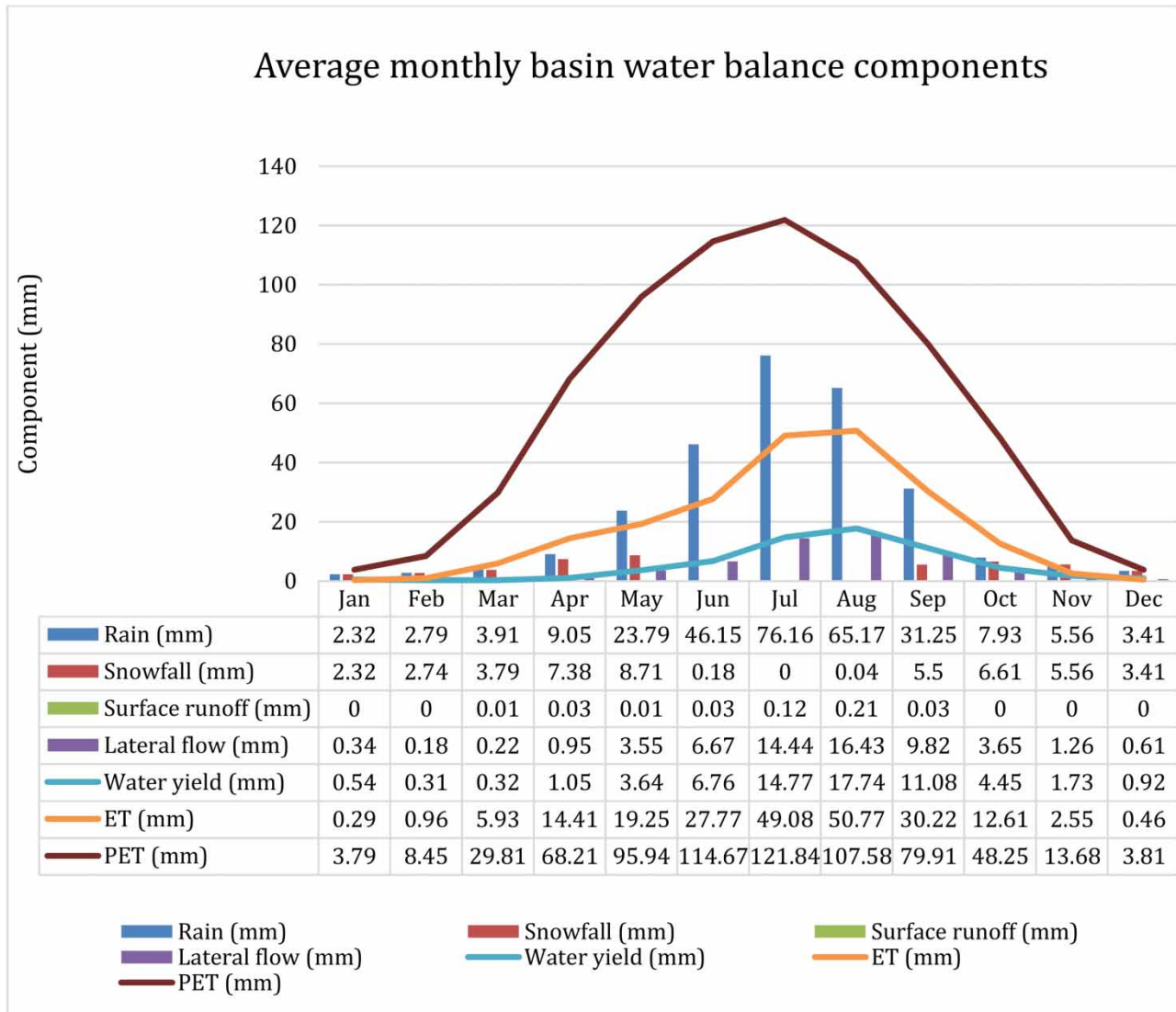


Figure 8 | Annual water balance components in the TR Basin.

May, demand for ET also increases rapidly. The highest potential ET was observed in July, after which the ET again decreased as air temperatures subsided as days get shorter.

The time series of average monthly discharge and monthly mean air temperature, and average monthly precipitation in the TR watershed are shown in Figure 9. According to the simulation results of the average monthly discharge values in the TR watershed, 1993–1995 was a wet year. Starting from 1996 onwards, the simulated discharge values are lower than the previous years due to the warmer temperature and lower precipitation.

The time series of monthly average discharge values at each subbasin in the TR watershed is provided in Figure 10. There is a decreasing trend of monthly discharge over the years since 1996. The seasonal average discharge values at each subbasin in the TR watershed are provided in Figure 11.

The annual average discharge at each subbasin is spatially represented in Figure 12. The discharge values increase along the river and reach their highest value in subbasin one, the whole basin outlet.

4. CONCLUSIONS

Water scarcity is a critical issue in semiarid, cold climate regions with increasing land use. Simulation of the spatial and temporal processes can help understand the factors influencing scarcity and inform decisions at a watershed scale. This study

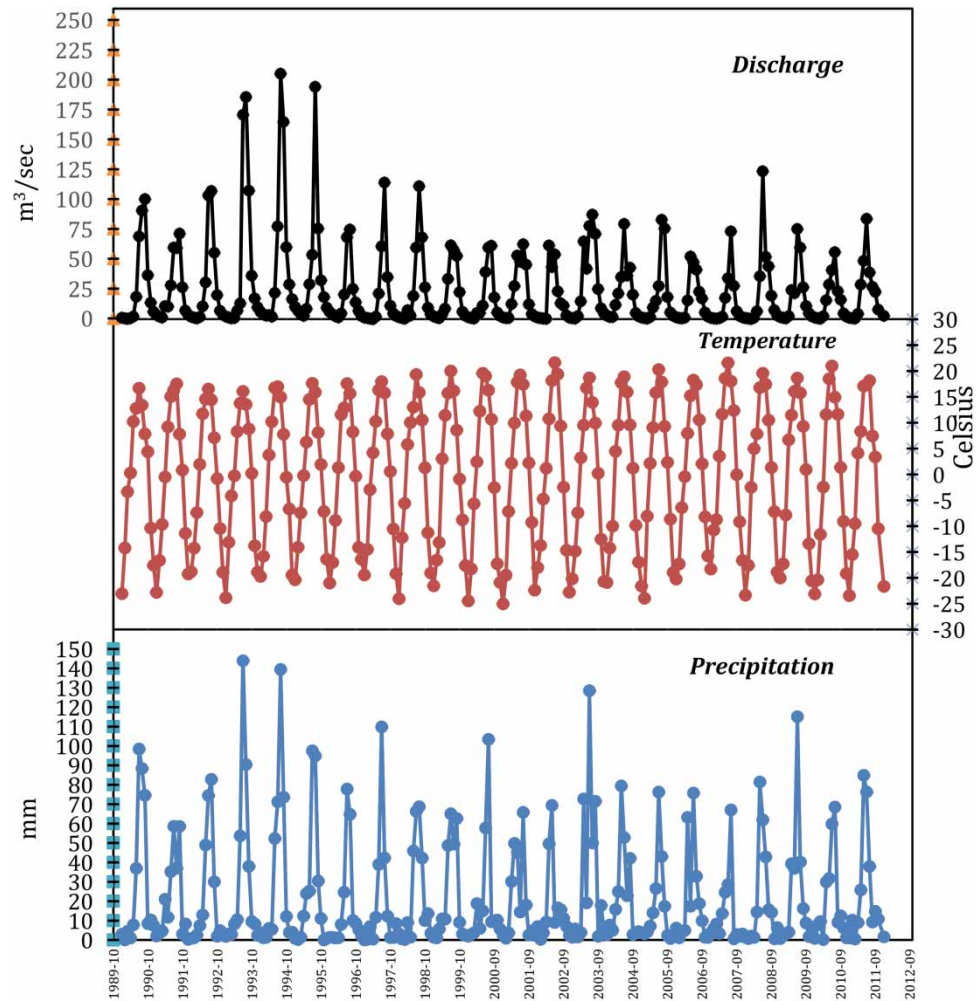


Figure 9 | Monthly average discharge, precipitation and mean air temperature values at TR Basin (1990–2011).

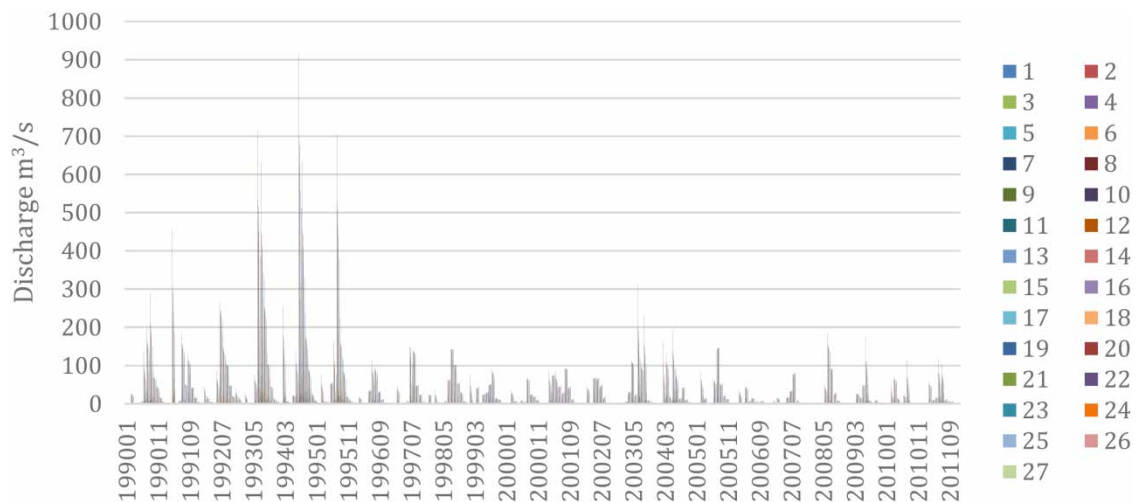


Figure 10 | Time series of monthly average discharge values at each subbasin in the TR watershed.

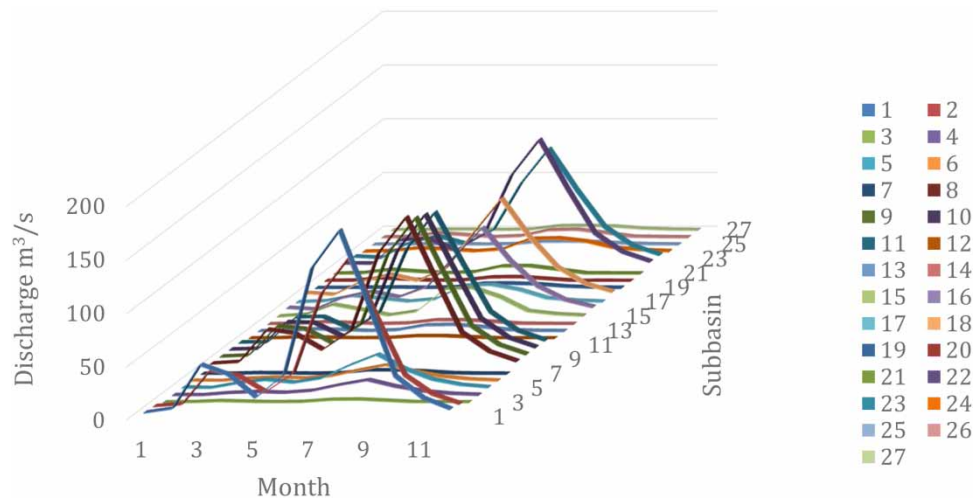


Figure 11 | Annual average discharge m^3/s at each subbasin outlets in the TR Basin.

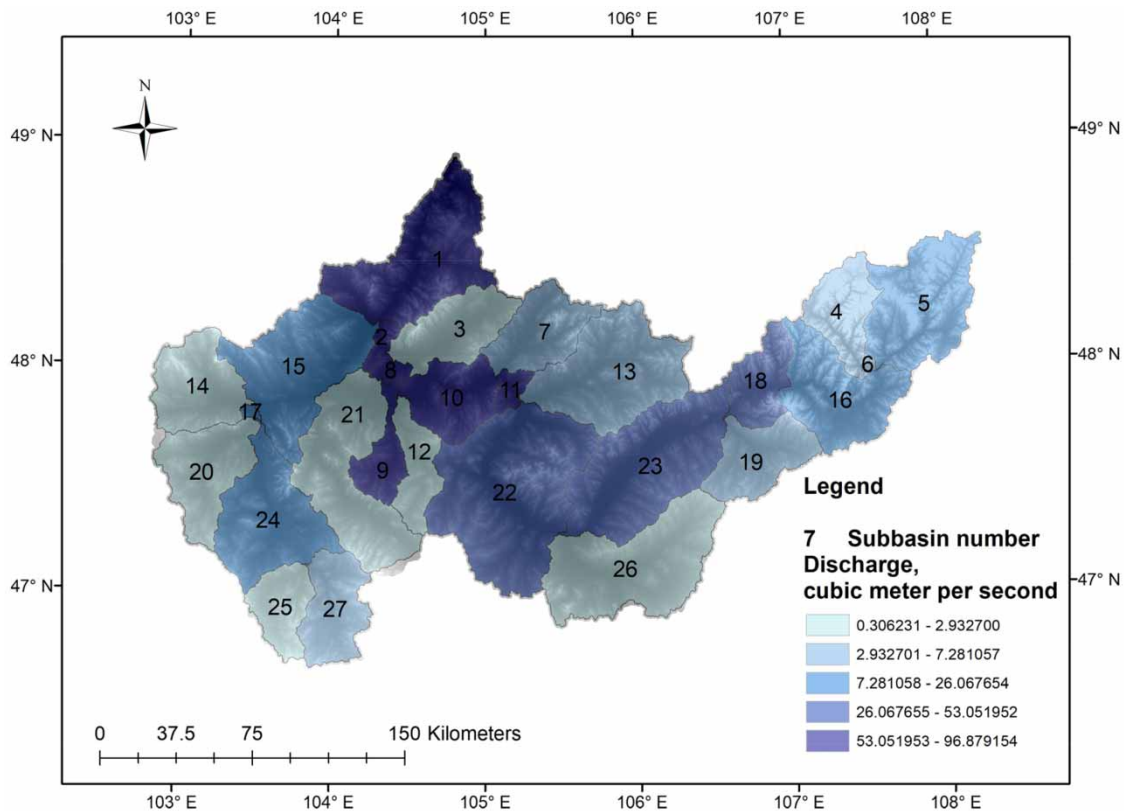


Figure 12 | Average discharge m^3/s at each subbasin outlets in the TR Basin.

contributes to the literature in simulating the dynamics to evaluate spatial and temporal patterns in the semiarid TR watershed less studied. Furthermore, the results will help manage water scarcity at a watershed scale for changing land-use conditions.

The SWAT model has performed well in simulating hydrologic processes in large watersheds worldwide. The model was used to simulate the watershed processes in the TR watershed with unique climatic and geomorphic conditions. Split-location, calibration, and validation are performed for monthly time-steps using observation at Terelj and Ulaanbaatar

stations. Calibration and validation were conducted with SUFI2 within SWAT-CUP methods using both graphical and statistical techniques. The R^2 , PBIAS, RSR, and NSE results demonstrate that the SWAT model effectively replicates annual, monthly streamflow values. In addition, we observe that the simulation model reasonably captures the watershed processes in the TR watershed.

Spatial and temporal variations in the streamflow discharge for the TR watershed were observed in the model simulation. The annual average discharge ranged from 0.3 to 96.87 m³/s in the basin, indicating a sizeable inter-annual variation in water flows. With water supplies facing high uncertainty, there is a need for watershed-wide management of water supplies and demand. The river flow was primarily influenced by climatic influences through precipitation and air temperature changes. This emphasizes the role of climate change in affecting the watershed hydrologic processes. With high actual ET in the watershed, decreasing river flows. We observe that spatial and temporal variations in hydrologic components are significant in the TR watershed.

The variability over geographic space and time is a fundamental issue in water management for scarcity. The methods and results of this study will be helpful for replication in similar semiarid watersheds elsewhere for addressing water scarcity at a watershed scale. In addition, information on variations over space can be used to target specific subwatersheds to address water scarcity issues.

The study has some limitations as it depends on the monitoring information for the calibration and validation of the simulation model. Data availability is often a major limitation in watersheds like TR, and future extensions can focus on developing and incorporating new datasets in the region. Other study extensions could quantify uncertainty in the area resulting from land use and climate change on watershed processes.

ACKNOWLEDGEMENTS

We thank the US Fulbright Program for providing the scholarship to pursue this research. Partial support is provided by NIFA-USDA, Massachusetts Agricultural Experiment Station (MAES) under projects MAS00036, MAS00035. We thank Dr David Bloniarz for his advice in the research.

DATA AVAILABILITY STATEMENT

All relevant data are available from publicly available datasets listed in methods (Table 1).

REFERENCES

- Abbaspour, K. C., Vejdani, M., Haghighat, S. & Yang, J. 2007 SWAT-CUP calibration and uncertainty programs for SWAT. In: *MODSIM 2007 International Congress on Modelling and Simulation, Modelling and Simulation Society of Australia and New Zealand* (Oxley, L. & Kulasiri, D., eds), pp. 1596–1602. Available from: https://www.mssanz.org.au/MODSIM07/papers/24_s17/SWAT-CUP_s17_Abbaspour_.pdf (accessed December 2016).
- Abbaspour, K. C., Rouholahnejad, E., Vaghefi, S., Srinivasan, R., Yang, H. & Kløve, B. 2015 A continental-scale hydrology and water quality model for Europe: calibration and uncertainty of a high-resolution large-scale SWAT model. *Journal of Hydrology* **524**, 733–752. <https://doi.org/10.1016/j.jhydrol.2015.03.027>.
- Abouabdillah, A., White, M., Arnold, J. G., De Girolamo, A. M., Oueslati, O., Maataoui, A. & Lo Porto, A. 2014 Evaluation of soil and water conservation measures in a semiarid river basin in Tunisia using SWAT. *Soil Use and Management* **30**, 539–549. <https://doi.org/10.1111/sum.12146>.
- Arino, O., Ramos, P., Jose, J., Kalogirou, V., Bontemps, S., Defourny, P. & Van Bogaert, E. 2012 Global Land Cover Map for 2009 (GlobCover 2009). European Space Agency (ESA) & Université catholique de Louvain (UCL), PANGAEA, <https://doi.org/10.1594/PANGAEA.787668>.
- Arnold, J. G., Srinivasan, R., Muttiah, R. S. & Williams, J. R. 1998 Large area hydrologic modeling and assessment part I: model development. *Journal of the American Water Resources Association* **34**, 73–89. <https://doi.org/10.1111/j.1752-1688.1998.tb05961.x>.
- Arnold, J. G., Muttiah, R. S., Srinivasan, R. & Allen, P. M. 2000 Regional estimation of base flow and groundwater recharge in the Upper Mississippi river basin. *Journal of Hydrology* **227** (1–4), 21–40.
- Arnold, J. G., Moriasi, D. N., Gassman, P. W., Abbaspour, K. C., White, M. J., Srinivasan, R., Santhi, C., Harmel, R. D., van Griensven, A., Van Liew, M. W., Kannan, N. & Jha, M. K. 2012 SWAT: model use, calibration, and validation. *Transactions of the ASABE* **55** (4), 1491–1508. <https://doi.org/10.13031/2013.42256>.
- Beven, K. & Binley, A. 1992 The future of distributed models: model calibration and uncertainty prediction. *Hydrological Processes* **6** (3), 279–298. <https://doi.org/10.1002/hyp.3360060305>.

- Boithias, L., Sauvage, S., Lenica, A., Roux, H., Abbaspour, K. C., Larnier, K., Dartus, D. & Sánchez-Pérez, J. M. 2017 *Simulating flash floods at hourly time-step using the SWAT model*. *Water* **9** (12), 929. <https://doi.org/10.3390/w9120929>.
- Dalai, S., Dambaravjaa, O. & Purevjav, G. 2019 *Water Challenges in Ulaanbaatar, Mongolia. Urban Drought*. Springer, Singapore, pp. 347–361. https://doi.org/10.1007/978-981-10-8947-3_20.
- Dessu, S. B., Melesse, A. M., Bhat, M. G. & McClain, M. E. 2014 *Assessment of water resources availability and demand in the Mara River Basin*. *CATENA* **115**, 104–114. <https://doi.org/10.1016/j.catena.2013.11.017>.
- Devia, G. K., Ganasri, B. P. & Dwarakish, G. S. 2015 *A review on hydrological models*. *Aquatic Procedia* **4**, 1001–1007. <https://doi.org/10.1016/j.aqpro.2015.02.126>.
- Dharmaratna, D. & Harris, E. 2012 *Estimating residential water demand using the Stone-Geary functional form: the case of Sri Lanka*. *Water Resources Management* **26**, 2283–2299. <https://doi.org/10.1007/s11269-012-0017-1>.
- Dolgorsuren, G., Chagnaa, N., Gerelchuluun, J., Puntsagsuren, C., Linden, W., Bakey, A., Dalai, J., Borchuluun, U., Davaa, G., Oyunbaatar, D., Jadambaa, N., Demeusy, J., Baldangombo, I., Tumurchudur, S., Khishigsuren, P., Batjargal, D., Tsogzolmaa, K., Davaanyam, T. & Odsuren, B. 2012 *Tuul River Basin Integrated Water Resources Management Assessment Report*. Ministry of Environment and Green Development, Ulaanbaatar, Mongolia. Available from: <http://extwprlegs1.fao.org/docs/pdf/mon169814.pdf> (accessed September 2016)
- Douglas-Mankin, K. R., Srinivasan, R. & Arnold, J. G. 2010 *Soil and Water Assessment Tool (SWAT) model: current developments and applications*. *Transactions of the ASABE* **53** (5), 1423–1431. <https://doi.org/10.13031/2013.34915>.
- Fan, M. & Shibata, H. 2015 *Simulation of watershed hydrology and stream water quality under land use and climate change scenarios in Teshio River watershed, northern Japan*. *Ecological Indicators* **50**, 79–89. <https://doi.org/10.1016/j.ecolind.2014.11.003>.
- Faramarzi, M., Abbaspour, K. C., Adamowicz, W. L., Lu, W., Fennell, J., Zehnder, A. J. B. & Goss, G. G. 2017 *Uncertainty based assessment of dynamic freshwater scarcity in semiarid watersheds of Alberta, Canada*. *Journal of Hydrology: Regional Studies* **9**, 48–68. <https://doi.org/10.1016/j.ejrh.2016.11.003>.
- Ficklin, D. L., Luo, Y. & Zhang, M. 2013 *Watershed modelling of hydrology and water quality in the Sacramento River watershed*. *California* **27**, 236–250. <https://doi.org/10.1002/hyp.9222>.
- Fiseha, B. M., Setegn, S. G., Melesse, A. M., Volpi, E. & Fiori, A. 2013 *Hydrological analysis of the Upper Tiber River Basin, Central Italy: a watershed modelling approach*. *Hydrologic Processes* **27**, 2339–2351. <https://doi.org/10.1002/hyp.9234>.
- Fukunaga, D. C., Cecilio, R. A., Zanetti, S. S., Oliveira, L. T. & Caiado, M. A. C. 2015 *Application of the SWAT hydrologic model to a tropical watershed at Brazil*. *CATENA* **125**, 206–213. <https://doi.org/10.1016/j.catena.2014.10.032>.
- Gassman, P. W., Reyes, M. R., Green, C. H. & Arnold, J. G. 2007 *The soil and water assessment tool: historical development, applications, and future research directions*. *Transactions of the ASABE* **50** (4), 1211–1250. <https://doi.org/10.13031/2013.23637>.
- Hongfu, M., Jing, L., Jing, W., Cui, Q. & Ke, F. 2012 *Simulation of eco-hydrological process in Hani Terrace wetland*. *Procedia Earth and Planetary Science* **5**, 230–236. <https://doi.org/10.1016/j.proeps.2012.01.040>.
- Hülsmann, L., Geyer, T., Schweitzer, C., Priess, J. & Karthe, D. 2015 *The effect of subarctic conditions on water resources: initial results and limitations of the SWAT model applied to the Kharaa River Basin in Northern Mongolia*. *Environmental Earth Sciences* **73**, 581–592. <https://doi.org/10.1007/s12665-014-3173-1>.
- Japan International Cooperation Agency. 2010 *Preparatory Survey Report on the Ulaanbaatar Water Supply Development Project in Gachuurt in Mongolia*. Japan International Cooperation Agency: CTI Engineering International Co., Ltd, Tokyo, Japan. Available from: https://openjicareport.jica.go.jp/pdf/11999612_01.pdf (accessed June 2017).
- Johannsen, I., Hengst, J., Goll, A., Höllermann, B. & Dieckkrüger, B. 2016a *Future of water supply and demand in the Middle Drâa Valley, Morocco, under climate and land use change*. *Water* **8**, 313. <https://doi.org/10.3390/w8080313>.
- Jujnovsky, J., Ramos, A., Caro-Borrero, Á., Mazari-Hiriart, M., Maass, M. & Almeida-Leñero, L. 2017 *Water assessment in a peri-urban watershed in Mexico City: a focus on an ecosystem services approach*. *Ecosystem Services* **24**, 91–100. <https://doi.org/10.1007/s10113-014-0742-5>.
- Khalid, K., Ali, M. F., Abd Rahman, N. F., Mispan, M. R., Haron, S. H., Othman, Z. & Bachok, M. F. 2016 *Sensitivity analysis in watershed model using SUFI-2 algorithm*. *Procedia Engineering* **162**, 441–447. <https://doi.org/10.1016/j.proeng.2016.11.086>.
- Krysanova, V. & Srinivasan, R. 2015 *Assessment of climate and land use change impacts with SWAT*. *Regional Environmental Change* **15** (3), 431–434. <https://doi.org/10.1007/s10113-014-0742-5>.
- Lindenschmidt, K. E. & Rokaya, P. 2019 *A stochastic hydraulic modelling approach to determining the probable maximum staging of ice-jam floods*. *Journal of Environmental Informatics* **34** (1). <https://doi.org/10.3808/jei.201900416>.
- Marshall, E. & Randhir, T. 2008 *Effect of climate change on watershed system: a regional analysis*. *Climatic Change* **89** (3), 263–280. <https://doi.org/10.1007/s10584-007-9389-2>.
- Monteith, J. L. 1965 *Evaporation and environment*. In Symp. Soc. Exp. Biol. (19, 205–23). Available from: <https://repository.rothamsted.ac.uk/download/8ae229c1c0ea4f617750d8e98d2ee6c356c306fc01a39bb584a18eb112f443e1/3879831/Monteith65.pdf> (accessed September 2016).
- Moriasi, D. N., Arnold, J. G., Van Liew, M. W., Bingner, R. L., Harmel, R. D. & Veith, T. L. 2007 *Model evaluation guidelines for systematic quantification of accuracy in watershed simulations*. *American Society of Agricultural and Biological Engineers* **50** (3), 885–900. <https://doi.org/10.13031/2013.23153>.
- NASA JPL 2009 *ASTER Global Digital Elevation Model [Data set]*. NASA JPL. Available from: <https://asterweb.jpl.nasa.gov/gdem.asp> (accessed September 2016).

- Nash, J. E. & Sutcliffe, J. V. 1970 River flow forecasting through conceptual models: part 1. A discussion of principles. *Journal of Hydrology* **10** (3), 282–290. [https://doi.org/10.1016/0022-1694\(70\)90255-6](https://doi.org/10.1016/0022-1694(70)90255-6).
- Neupane, R. & Kumar, S. 2015 Estimating the effects of potential climate and land use changes on hydrologic processes of a large agriculture dominated watershed. *Journal of Hydrology* **529**, 418–429. <https://doi.org/10.1016/j.jhydrol.2015.07.050>.
- Niu, G., Troch, P. A., Paniconi, C., Scott, R. L., Durcik, M., Zeng, X., Huxman, T., Goodrich, D. & Pelletier, J. 2014 An integrated modeling framework of catchment-scale ecohydrological processes: 2. The role of water subsidy by overland flow on vegetation dynamics in a semiarid catchment. *Ecohydrology* **7**, 815–827. <https://doi.org/10.1002/eco.1405>.
- Nohegar, A., Malekian, A., Hosseini, M., Holisaz, A. & Taghvaye, S. E. 2017 Comparison of SUFI-2 AND GLUE algorithms on runoff simulations in forest catchments: a case study in the Shafaroud Catchment. *Watershed Engineering and Management* **8** (4), 389–399.
- Pietroń, J., Jarsjö, J., Romanchenko, A. O. & Chalov, S. R. 2015 Model analyses of the contribution of in-channel processes to sediment concentration hysteresis loops. *Journal of Hydrology* **527**, 576–589. <https://doi.org/10.1016/j.jhydrol.2015.05.009>.
- Sajikumar, N. & Remya, R. S. 2015 Impact of land cover and land use change on runoff characteristics. *Journal of Environmental Management* **161**, 460–468. <https://doi.org/10.1016/j.jenvman.2014.12.041>.
- Santhi, C., Arnold, J. G., Williams, J. R., Dugas, W. A., Srinivasan, R. & Hauck, L. M. 2001 Validation of the SWAT model on a large river basin with point and nonpoint sources. *Journal of the American Water Resources Association* **37** (5), 1169–1188. <https://doi.org/10.1111/j.1752-1688.2001.tb03630.x>.
- Sukhbaatar, C., Sajjad, R. U., Luntun, J., Yu, S. & Lee, C. 2017 Climate change impact on the Tuul River flow in a Semiarid region in Mongolia. *Water Environment Research* **89**, 527–538. <https://doi.org/10.2175/106143016X14798353399223>.
- Talib, A. & Randhir, T. O. 2017 Climate change and land use impacts on hydrologic processes of watershed systems. *Journal of Water and Climate Change* **8** (3), 363–374. <https://doi.org/10.2166/wcc.2017.064>.
- Tsujimura, M., Ikeda, K., Tanaka, T., Janchivdorj, L., Erdenechimeg, B., Unurjargal, D. & Jayakumar, R. 2013 Groundwater and surface water interaction in an Alluvial Plain, Tuul River Basin, Ulaanbaatar, Mongolia. *Sciences in Cold Arid Regions* **5** (1), 126–132. <https://doi.org/10.3724/SP.J.1226.2013.00126>.
- Tsvetkova, O. & Randhir, T. O. 2019 Spatial and temporal uncertainty in climatic impacts on watershed systems. *Science of the Total Environment* **687**, 618–633. <https://doi.org/10.1016/j.scitotenv.2019.06.141>.
- United Nations 2019 *2019 Revision of World Population Prospects*. Population Division, United Nations, NY, USA. Available from: <https://population.un.org/wpp/> (accessed 21 April 2021).
- USDA-SCS 1972 *National Engineering Handbook, Section 4: Hydrology*. USDA-SCS, Washington, DC.
- USDA 1983 *National Engineering Handbook, Hydrology Section 4*. USDA-SCS, Washington, DC, Chapter 19.
- Wang, G., Yang, H., Wang, L., Xu, Z. & Xue, B. 2014 Using the SWAT model to assess impacts of land use changes on runoff generation in headwaters. *Hydrological Processes* **28** (3), 1032–1042. <https://doi.org/10.1002/hyp.9645>.
- Wang, F., Huang, G. H., Fan, Y. & Li, Y. P. 2020 Robust subsampling ANOVA methods for sensitivity analysis of water resource and environmental models. *Water Resources Management* **34** (10), 3199–3217. <https://doi.org/10.1007/s11269-020-02608-2>.
- Wang, F., Huang, G. H., Cheng, G. H. & Li, Y. P. 2021a Multi-level factorial analysis for ensemble data-driven hydrological prediction. *Advances in Water Resources* 103948. <https://doi.org/10.1016/j.advwatres.2021.103948>.
- Wang, F., Huang, G. H., Fan, Y. & Li, Y. P. 2021b Development of clustered polynomial chaos expansion model for stochastic hydrological prediction. *Journal of Hydrology* **595**, 126022. <https://doi.org/10.1016/j.jhydrol.2021.126022>.

First received 21 April 2021; accepted in revised form 28 July 2021. Available online 10 August 2021